

## Error Estimation of Measured Exhaust Gas Temperature in Afterburner Mode in an Aero Gas Turbine Engine

Benny George\* and N. Muthuveerappan

*DRDO-Gas Turbine Research Establishment, Bangalore - 560 093, India*

*\*E-mail: bennygeorge@gtre.drdo.in*

### ABSTRACT

In a turbofan engine, thrust is a key parameter which is measured or estimated from various parameters acquired during engine testing in an engine testbed. Exhaust gas temperature (EGT) is the most critical parameter used for thrust calculation. This work presents a novel way to measure and correct the errors in EGT measurement. A temperature probe is designed to measure EGT in the engine jet pipe using thermocouples. The temperature probe is designed to withstand the mechanical and temperature loads during the operation. Structural analysis at the design stage provided a strength margin of 90% and eigenfrequency margin of more than 20%. Thermal analysis is carried out to evaluate maximum metal temperature. Errors are quite high in high-temperature measurements which are corrected using the available methodologies. The velocity error, conduction error, and radiation error are estimated for the measured temperature. The difference of 97 K between the measured gas temperature and calculated gas temperature from measured thrust is explained. The estimated velocity error is 1 K, conduction error is 3 K, and radiation error is 69 K. Based on the error estimation, the measurement error is brought down to 24 K. After applying the above corrections, the further difference of 24 K between measured and estimated value can be attributed to thermocouple error of +/-0.4% of the reading for class 1 accuracy thermocouple, other parameter measurement errors, and analysis uncertainties. The present work enables the designer to calculate the errors in high-temperature measurement in a turbofan engine.

**Keywords:** Turbofan engine; EGT; Probe design; Analysis; Velocity error; Conduction error; Radiation error

### NOMENCLATURE

EGT	Exhaust gas temperature	$M_j$	Thermocouple junction Mach number
CFD	Computational fluid dynamics	$M_F$	Free stream Mach number
GC	Acceleration due to gravity	$A_E$	Area entry Kiel
$T$	Temperature	$A_B$	Area bleed hole
$P$	Pressure	$\gamma$	Ratio of specific heats
$\sigma_b$	Bending stress	$V_E$	Velocity error
NH	High-pressure compressor speed	$R$	Recovery factor
NL	Low-pressure compressor speed	$C_E$	Conduction error
$R_N$	Reynolds number	$T_M$	Temperature mount
$Tu$	Turbulence intensity	$L$	Length of thermocouple exposed
$P_N$	Prandtl number	$D$	Diameter of thermocouple
$Nu$	Nusselt number	$k_s$	Thermal conductivity of thermocouple
$h_c$	Convective heat transfer coefficient	$\rho$	Density of gas
$d$	Diameter of cooling hole	$V$	Velocity of gas
$k_g$	Thermal conductivity of the gas	$\mu$	Absolute viscosity of the gas
$F_x$	Thrust	$R_E$	Radiation error
$M_F$	Mass flow	$\sigma$	Stefan Boltzmann constant
$V_j$	Velocity of jet	$\epsilon$	Emissivity of thermocouple
$V_a$	Velocity of aircraft	$T_w$	Temperature wall
$P_s$	Static pressure		
$P_a$	Ambient pressure		
$A_N$	Area of the nozzle		
$T_j$	Thermocouple Junction Temperature		
$T_T$	Total temperature		
$T_S$	Static temperature		
$T/C$	Thermocouple		

### 1. INTRODUCTION

In a turbofan engine, gas temperature and pressure are the two critical parameters measured to ensure operability and performance at all speeds. These two parameters measured at the exit of the low-pressure turbine dictate the thrust output of an engine in dry and afterburner mode. The afterburner mode is engaged when the thrust requirement of the engine is to be enhanced for a short while to the extent of 50%<sup>1</sup>. In-flight

thrust measurement is not feasible, hence EGT measurement in afterburner mode is used to evaluate the thrust. EGT goes as high as 2000 K or beyond in afterburner mode based on the engine configuration<sup>2</sup>. Infrared (IR) suppression systems in the latest stealth aircraft also require EGT measurement to know the wavelength of emitted IR radiation from the aircraft engine<sup>3</sup>.

There are various non-contact and contact methods available to measure such a high temperature. One of the most common non-contact methods is using IR (Infrared) based probes. IR probes are best suited for surface temperature measurement. Kerr<sup>4</sup>, *et al.* describes pyrometer design and therefore temperature measurement as a trade-off between various parameters. These parameters are classified under two categories. The first category covers the target related properties viz., the target size, target material properties, and the target emissivity. The second category includes temperature measurement range, accuracy of calibration, nature of optical path, and resolution. Among all the properties mentioned above, the emittance of the target is the most critical parameter, which needs to be measured with reasonable accuracy. As many parameters are involved in accurately predicting the emission coefficient of the target surface, it makes the measurement more complex and difficult<sup>5</sup>. Another non-contact method in high-temperature measurement is using TDLAS (Tunable Diode Laser Absorption Spectroscopy) which works on the principle of laser interferometry<sup>6</sup>. The associated measurement problems are laser noise, drifts, general interferometric effects, and stability problems. So accurate measurement of high temperature using non-contact methods is very complex and the error can go as high as 10% when compared to the error of 2% in contact methods<sup>7</sup>.

The above measurement problems are overcome by using contact method measurement with a noble metal thermocouple-based air-cooled probe which is presented in this paper. Even though measurement errors are present in both methods, more accurate prediction of errors is possible with the contact method. In the contact method, the probe design depends on many inlet parameters to which the probe is subjected. The structural integrity of the probe has been ensured during the design phase itself by carrying out the finite element analysis. CFD analysis using different turbulence models for predicting gas temperature distribution in scram-jet engines was carried out by various researchers<sup>8,9,10</sup>. A Kiel houses the sensing element which faces the gas flow. Researchers have earlier carried out the design and development of temperature probes for temperature measurement up to 1000 K using contact method highlighting the associated problems<sup>11,12,13</sup>. Recent works of literature are more oriented towards using pyrometers for high-temperature measurements<sup>14</sup>. Various studies have been carried out by researchers to optimise stagnation tube geometries in temperature and pressure measurements<sup>15,16,17</sup>. Even though the above works of literature cover the measurement aspects and associated measurement problems while using thermocouple-based probes, the error estimation part is not addressed for high-temperature application. The novelty in the present work lies in design, development of a contact probe, and successful measurement of EGT followed by estimating the errors in

high-temperature measurement above 1000 K. Probe design is customised based on the measurement requirements and space available at the station where it is mounted inside the gas turbine engine. The present work highlights the problems associated with the design and development of a high-temperature probe for measuring gas temperature in afterburner mode followed by error estimation in a turbofan engine.

## 2. TEMPERATURE PROBE DESIGN

The probe is a cantilever and two sensors are placed inside the probe body. One sensor is used to measure the gas total temperature and another sensor is used to measure probe body temperature as shown in Fig. 1. The diameter of the probe is decided by the size of the sensors and the size of the cooling airflow path. The probe is installed on the flow path of the engine and faces the hot gas in the afterburner mode. The stagnation tube of the probe houses an ungrounded R-type thermocouple of 1.0 mm diameter sheath to measure the gas temperature. Probe body temperature is measured by another R-type thermocouple of 1.0 mm sheath diameter, which is located 45 mm above the gas temperature sensor inside the probe body. The material of the probe body is Haynes 188 which is an alloy of Co-Ni-Cr-W and it can withstand the temperature of the order of 1500 K.

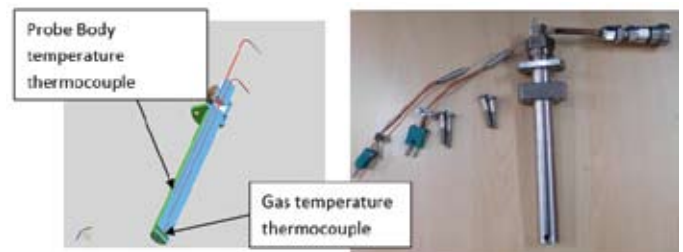


Figure 1. Air-cooled EGT probe.

### 2.1 Stress Analysis for Gas Loads

Stress analysis is carried out during the design phase of the probe to find out the maximum stress that acts on the probe body. The probe design is analysed using the finite element method in ANSYS R14.5 considering the gas load<sup>18</sup>. For analysis, the gas load acting on the probe in afterburner mode was taken as 275 kPa, and cooling air pressure as 710 kPa. The dynamic Young's Modulus of material corresponding to the gas temperature is taken as 150 GPa. The structural analysis of the probe showed a maximum Von Mises stress of 2.8 MPa on the probe body as shown in Fig. 2. The allowable material stress corresponding to the maximum allowable metal temperature is 28 MPa. It is assumed that material properties are isotropic, displacements are very small and parameters of structure are not changing under loading. Therefore, finite element analysis provided a strength margin of 90% for the probe stem in the design phase, thereby ensuring the mechanical integrity of the probe.

### 2.2 Eigenvalue Analysis of the Probe

Eigenvalue analysis of the probe was carried out to find the first few natural frequencies. Higher-order frequencies are usually discarded as they will not interfere with the first

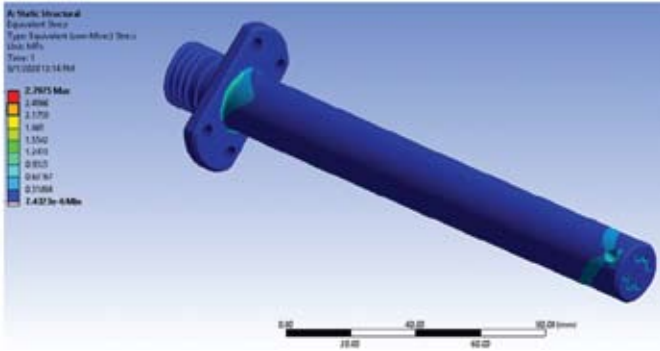


Figure 2. Finite element analysis stress plot.

3 engine orders. These natural frequencies are cross-referred with the first 3 engine orders for any possible interference. Figure 3 shows the first fundamental natural frequency of 432 Hz corresponding to the first bending mode which is well outside the margin requirement of 20%<sup>19</sup>.

Campbell diagram based on eigenvalue analysis gives possible interference of probe natural frequencies with the first 3 engine orders. The Campbell diagram generated shows that the first engine order (EO) is cleared with all probe natural frequencies. First flexural and first transverse mode interference with higher engine order happens at lower speed cross-overs. The nearest blade pass frequency, which is 12530 Hz is well above the first 3 engine orders. Figure 4 shows the Campbell diagram generated based on eigenvalue analysis.

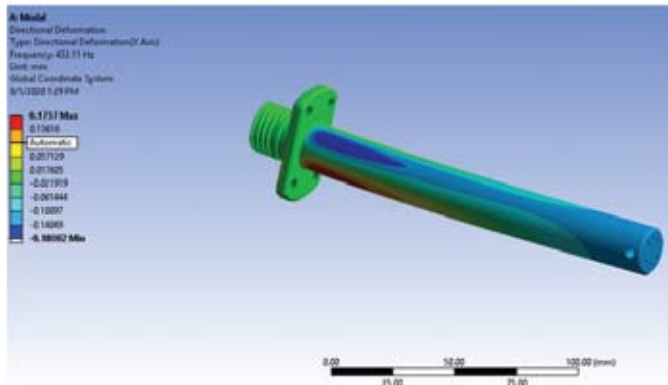


Figure 3. Eigenvalue analysis plot.

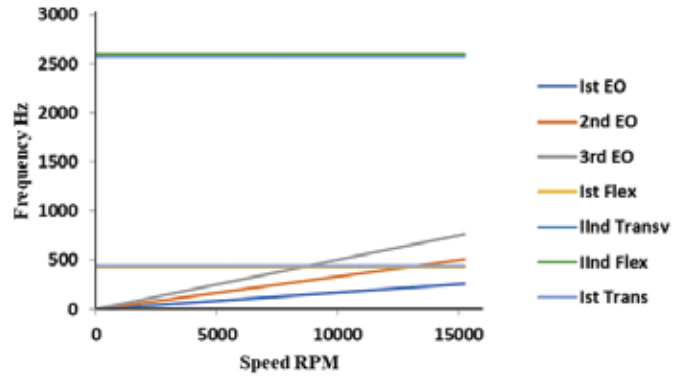


Figure 4. Campbell diagram based on eigenvalue analysis.

### 2.3 CFD Analysis

CFD analysis was carried out using ANSYS R19 to obtain the gas temperature distribution at the inlet of the probe<sup>20</sup>. The jet pipe is modelled and the boundary conditions are simulated at the inlet and outlet of the jet pipe.

Table 1 shows the inlet and outlet boundary conditions applied for the CFD analysis:

Table 1. Inlet and outlet boundary conditions applied for the CFD analysis

Inlet pressure core	275 kPa
Inlet temperature core	1000 K
Inlet pressure bypass	280 kPa
Inlet temperature bypass	425 K
Afterburner fuel flow	50 Gpm
Equivalence ratio	1
Outlet pressure	91 kPa

The salient mesh qualities are minimum orthogonality of 0.1, the maximum aspect ratio of 10, and  $Y^+ < 5$ .

Turbulence intensity for core flow and bypass flow is 10% and 5 % respectively. Average swirl is taken as 8% estimated from upstream component design. The turbulence model is K- $\omega$  SST.

The turbulent viscosity is assumed to be isotropic.

Figure 5 shows the gas temperature distribution at the plane of measurement in the jet pipe and the graph shows the radial gas temperature distribution at three angular locations.

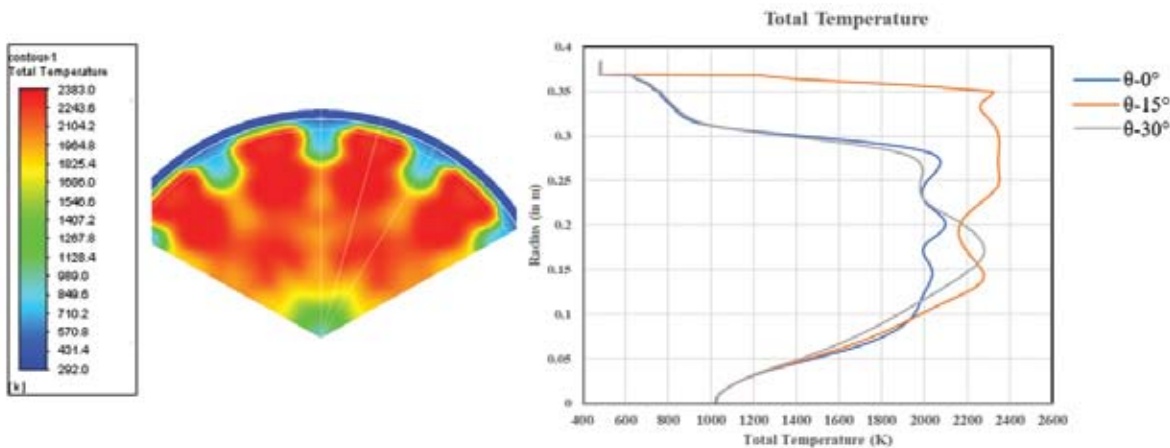


Figure 5. Gas temperature distribution in afterburner mode from CFD analysis.

This gas temperature is taken as an input for heat transfer analysis. The maximum gas temperature is of the order of 2100 K at the location of the probe.

**2.4 Heat Transfer Analysis**

The probe is air-cooled through six holes drilled on the probe body. Cooling air is supplied at a pressure of 710 kPa, and a temperature of 298 K. The size of each cooling hole is 2.0 mm and the air mass flow rate is 0.03 Kg/s. The external gas and cooling air circuit are shown in Fig. 6.

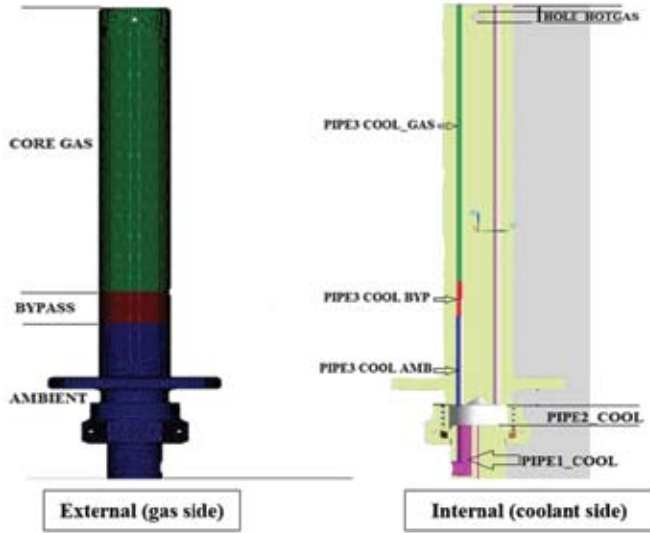


Figure 6. Arrangement of gas and coolant side for T7 probe.

Finite element heat transfer analysis is carried out to estimate the metal temperature of the probe. The coolant mass flow going through the channels is evaluated for the given openings. The heat loads coming on the probe are estimated using the standard correlations available in the open literature. Lowery and Vachon correlation is used to calculate the gas side convective heat transfer coefficient at the leading edge of the probe<sup>21</sup>.

$$Nu = \sqrt{R_N} * \left[ \left( 1.01 + 2.624 * Tu * \frac{\sqrt{R_N}}{100} \right) - 3.07 \left( Tu * \frac{\sqrt{R_N}}{100} \right)^2 \right] \tag{1}$$

The analysis is carried out for the maximum afterburner testbed condition. It is assumed that steady-state conditions are reached, one-dimensional heat transfer by conduction and convection, thermal conductivity is constant, heat transfer coefficient is uniform over the surface, and radiation heat transfer is neglected. The heat loads are estimated from the pressure, temperature, and velocities obtained from CFD analysis. Convective heat transfer coefficient is obtained using the following equation.

$$h_c = \frac{(Nu * k_g)}{d} \tag{2}$$

Convective heat transfer coefficients on the gas and coolant side are given for the heat transfer analysis and the analysis was carried out using ANSYS R19.

Flow parameters for heat transfer analysis are shown in Table 2.

Figure 7 shows the temperature distribution on the probe body from heat transfer analysis for the maximum afterburner testbed condition. The maximum metal temperature of the probe is 1558 K which can be allowed for short-term exposure.

**3. PROBE INSTALLATION ON ENGINE**

The probe houses an R-type thermocouple at a distance of 115 mm inside the jet pipe liner, downstream of the exhaust gas in the afterburner region as shown in Fig. 8. The probe is cooled using compressed air supplied at a pressure of 710 kPa and a temperature of 298 K. The probe body metal temperature is measured using another R-type thermocouple fixed on the probe stem at a distance of 45 mm from the gas temperature sensor. The typical response time of 1.0 mm diameter R type thermocouple with 0.15 mm thermocouple bead diameter is 0.15 seconds<sup>22</sup>. This measurement is used to verify probe body temperature distribution obtained from the heat transfer analysis. The measured body temperature is 1273 K whereas the heat transfer analysis shows a temperature of 1289 K.



Figure 7. Steady-state temperature distribution for temperature probe.



Figure 8. EGT Probe installed on the engine.

Table 2. Flow parameters for heat transfer analysis

Leading-edge of the probe			
Reynolds No	Turbulence intensity	HTC	Correlation
70000	5%	2000 W/m <sup>2</sup> K	Lowery & Vachon
Coolant side			
90000	Not applicable	1500 to 3700 W/m <sup>2</sup> K	Dittus-Boelter Correlation.

Applicability of the above correlations.

1. Lowery Vachon correlation: 0 < Tu \* sqrt(Re) < 64
2. DB Correlation: 0.7 ≤ Pr ≤ 160 Re ≥ 10000 L/D ≥ 10

The probe installed inside the engine jet pipe during one of the afterburner tests for measuring gas total temperature is shown in Fig. 8. The measured gas temperature, probe body temperature, fuel flow, and thrust are shown in Fig. 9.

The maximum gas temperature (T7 GAS) measured by the probe is 1800 K as shown in Fig. 9. The afterburner fuel flow is slowly increased from 6 GPM to 50 GPM in 5 to 6 steps. The maximum steady-state temperature measured at the end of the last step is 1800 K. The above value of measured total temperature ( $T_j$ ) needs to be corrected for measurement errors and compared with gas total temperature ( $T_T$ ) calculated from measured thrust. The gas total temperature is calculated from measured thrust using the following equation.

$$F_X = M_F * (V_j - V_a) + (P_s - P_a) * A_N \quad (3)$$

$$T_T = \frac{[(1.315 * TS * M_F) - (10 * 473)]}{61} \quad (4)$$

where  $V_j$  is a function of gas total temperature.  $T_T$  is derived from measured thrust, the velocity of jet, mass flow, and static pressures. From the measured thrust, the calculated gas total temperature  $T_T$  is 1897 K, which is in between the measured value and the CFD prediction. The uncertainty in  $T_T$  is +/- 0.65% which is derived from the measured parameter uncertainties. A difference of 97 K from the measured temperature can be attributed to measurement errors and other uncertainties.

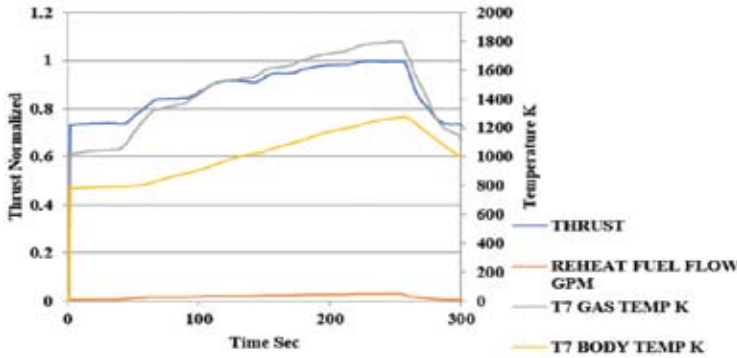


Figure 9. Measured EGT plot during afterburner test.

#### 4. ERROR ESTIMATION IN EGT MEASUREMENT

A difference of 97 K is observed between measured and calculated gas total temperature. The most important aerodynamic and thermodynamic factors affecting thermocouple probe design are velocity error, conduction error, and radiation error. The estimation of velocity error is fairly easy whereas estimation of conduction and radiation error is quite difficult as far as high-temperature measurements are concerned<sup>23</sup>. The radiation error is quite predominant with temperatures above 1000 K. Proper design of Kiel which houses the thermocouple plays a major role in minimizing the above errors.

##### 4.1 Velocity Error

Total temperature is the temperature measured when the flow is brought to rest adiabatically. This is an ideal

process and in practice, it is not feasible to bring the gas to rest adiabatically. As a result of this, the measured total temperature at thermocouple junction  $T_j$  will always show a lower value than the actual total temperature  $T_T$  of the gas. The Mach number inside the Kiel  $M_j$  at the thermocouple junction plays a major role in reducing the velocity error. This Mach number in turn depends on the free-stream Mach number  $M_F$ . Another major parameter influencing the thermocouple junction Mach number is the area ratio of the Kiel head inlet and the exit bleed holes. As the free-stream Mach number is an engine-related parameter, the only way to control the thermocouple junction Mach number is by controlling the inlet to exit area ratio. The velocity error can be minimised by reducing the Mach number of the internal flow  $M_j$  by controlling the inlet to exit area ratio. A higher inlet to exit ratio reduces the velocity error. A nearly linear relationship exists between free stream Mach number, Kiel's internal velocity, inlet to exit ratio, and thereby the velocity recovery factor. It is prudent to keep Kiel's internal Mach numbers between 0.05 and 0.15 to minimise the velocity recovery error in practical cases. In the present case of temperature measurement above 1000 K, radiation and conduction errors are very predominant which can be reduced by keeping the internal Mach number in the range of 0.15 to 0.2. Therefore, Kiel's internal Mach number is a trade-off between velocity error on one side and conduction and radiation error on the other side.

The inlet free-stream Mach number  $M_F$  for the present probe is calculated from the measured total and static pressure at the entry of the afterburner plane. For the calculated free-stream Mach number of 0.8, the variation of thermocouple junction Mach number  $M_j$  concerning Kiel entry ( $A_E$ ) to bleed hole ( $A_B$ ) area ratio is shown in Fig. 10.

Even though an  $A_E/A_B$  ratio of around 6 gives a junction Mach number  $M_j$  of 0.1, for measurement of high temperature slightly higher Mach number will reduce considerably the conduction and radiation error. The present probe is designed with an  $A_E/A_B$  ratio of 3.0 which gives a junction Mach number  $M_j$  of 0.19 derived from the following equation and shown in Fig. 10.

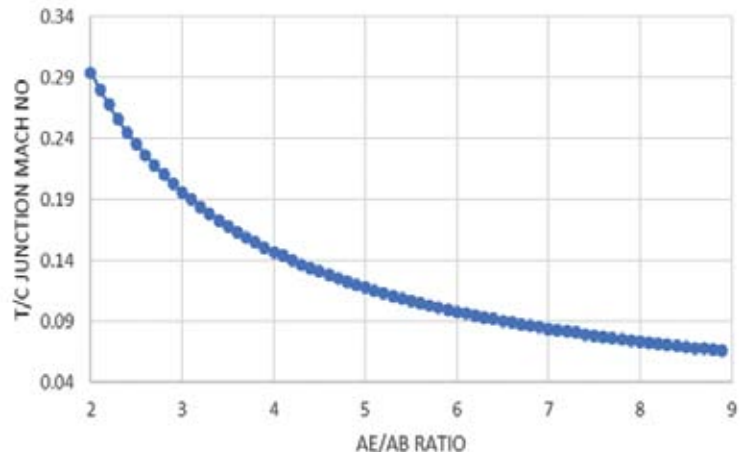


Figure 10. Thermocouple junction Mach no vs entry to bleed hole area ratio.

$$M_J = \frac{M_F}{\left(\frac{A_E}{A_B}\right)} \left[ 1 + \frac{\gamma-1}{2} M_F^2 \right]^{-\frac{1}{\gamma-1}} \quad (5)$$

The velocity recovery factor  $R$  for such a probe is of the order of 0.92 from the standard Kiel design<sup>24</sup>. The estimated temperature correction ( $V_E$ ) concerning velocity recovery for such a Kiel design is 1 K (0.05 %) as calculated from the following equation<sup>24</sup>.

$$V_E = (1-R) \left[ \frac{\frac{(\gamma-1)}{2} M_J^2}{1 + \frac{(\gamma-1)}{2} M_J^2} \right] T_T \quad (6)$$

#### 4.2 Conduction Error

It is assumed that the heat energy transferred from the hot gas to the thermocouple hot junction through forced convection is equal to the heat energy transferred through conduction along the thermocouple wire. The thermal energy loss due to conduction is given by the following equation<sup>24</sup>.

$$C_E = \frac{T_r - T_M}{\text{Cosh } L * \left[ \frac{4h_c}{D * k_s} \right]^{\frac{1}{2}}} \quad (7)$$

The conduction error  $C_E$  depends on the difference between gas temperature and probe wall temperature,  $L/D$  ratio of thermocouple, convective heat transfer coefficient, and thermal conductivity of thermocouple material. By increasing  $h_c$  (increasing thermocouple junction Mach number) and  $L/D$  ratio, conduction error can be reduced. The other two parameters are fixed.  $T_r$  is taken from calculated gas total temperature and  $T_M$  (1200 K) is taken heat transfer analysis.  $L/D$  ratio in the present probe design is kept as 2.5 mm due to limitations in probe geometry. The thermal conductivity  $k_s$  of thermocouple material is 100 W/mK. The convective heat transfer coefficient  $h_c$  is calculated from the Nusselt number which in turn is calculated from the Reynolds number.

For thermocouple normal to the flow, the Nusselt number is given by

$$Nu = (0.44 \pm 0.06)(R_N)^{0.5} \quad (8)$$

where,

$$\text{Reynolds number } R_N = \frac{(\rho * V * D)}{\mu} = 825 \quad (9)$$

where

$$\rho = 0.32 \text{ kg/m}^3$$

$$V = 155 \text{ m/s}$$

$$D = 0.001 \text{ m}$$

$$\mu = 6.01 * 10^{-5} \text{ kg/m-s}$$

$$Nu = 12.6$$

And convective heat transfer coefficient is given by

$$h_c = \left( \frac{Nu * k_g}{D} \right) = 1512 \quad (10)$$

where

$$k_g = 0.12 \text{ W/mK}$$

From the above, the conduction error is estimated as 3 K (0.15%).

#### 4.3 Radiation Error

Radiation error  $R_E$  is caused by radiation from the thermocouple junction to the Kiel enclosure. The error  $R_E$  of the thermocouple junction inside the Kiel enclosure is expressed by the equation<sup>24</sup>.

$$R_E = \frac{\sigma * \epsilon}{h_c} (T_T^4 - T_W^4) \quad (11)$$

where,

$$\sigma = 5.67 * 10^{-8} \text{ W/m}^2\text{K}^4$$

The emissivity of thermocouple,  $\epsilon$  is taken as 0.2<sup>25</sup>.  $T_W$  is taken as 1400 K from heat transfer analysis. Other than  $h_c$  all other parameters are fixed. The only way of reducing the radiation error is by increasing  $h_c$  (higher junction Mach number). The radiation error estimated from the above equation is 69 K (3.6%).

The total error in temperature measurement is calculated from three individual errors, namely velocity error, conduction error, and radiation error. As all these errors reduce the measured gas temperature, uncertainty analysis leads to the direct addition of all these errors to the measured value  $T_j$  to get the actual gas temperature  $T_T$ <sup>26</sup>. Based on the error estimation, the measurement error is brought down to 24 K.

#### 5. CONCLUSION

Thrust calculation calls for the measurement of EGT in a turbofan engine. Comparison is made between the measured and calculated gas total temperature during engine test in afterburner mode in the testbed. Error estimation of measured EGT using the high-temperature probe in afterburner mode is carried out. The design of probe is unique and customised for specific engine applications. Following inference is drawn from the present work:

- A probe using R-type thermocouples (for gas and body temperature measurement) was designed, developed, and used to measure the EGT in afterburner mode in a turbofan engine.
- Structural analysis of the probe ensured strength margin of 90% at maximum operating condition, thereby ensuring the mechanical integrity of the probe.
- Eigenvalue analysis was carried out to check the probe natural frequency interference with engine orders and margin was found above 20%.
- A steady-state heat transfer analysis was carried out to check the metal temperature distribution on the probe body with inputs taken from CFD analysis. The heat transfer analysis showed a maximum metal temperature of 1558 K.
- From exhaust gas temperature measurement, a difference of 97 K was noticed between the calculated and measured value of gas temperature. Further, the major errors in high-temperature measurement i.e., velocity error, conduction error, and radiation error were estimated. For

the given inlet condition, velocity error is estimated as 1 K, conduction error is estimated as 3 K, and radiation error is estimated as 69 K. The most predominant error in high-temperature measurement is radiation error which increases exponentially above 1000 K. Based on the error estimation of the measured temperature, the measurement difference is brought down to 24 K. This difference of 24 K still needs to be answered which can be attributed to thermocouple error which is +/-0.4% of the reading for class 1 accuracy thermocouple, signal conditioner errors, other parameter measurement errors, and analysis uncertainties.

- The methodology adopted in this paper for high-temperature probe design and estimation of errors in high-temperature measurement can be used as a guideline for designing similar probes and estimating the errors in a turbofan engine.
- There is further scope of work by considering catalytic error, thermocouple junction errors, thermocouple drift, parametric variation study, probe geometry optimisation, etc in high-temperature measurement.

## REFERENCES

1. Ebrahimi, H. B. Overview of Gas Turbine Augmentor Design Operation and Combustion Oscillation. AIAA 2006-4916. *In* 42nd AIAA/ASME/SAE/ASEE Joint Propulsion Conference & Exhibit, 9 - 12 July 2006, Sacramento, California.
2. Divya, M. S; Ganesan, S. & Mallikarjun, U. S. Conjugate Heat Transfer Analysis of Gas Turbine Afterburner System. *In* Int. Conf. on Advanced Materials, Manufacturing, Management & Thermal Sciences, May 03-04, 2013, ISBN-13 978-81-926304-0-3.
3. Baranwal, Nidhi & Mahulikar, S. P. Review of Infrared signature suppression systems using optical blocking method. *Defence Technology*, 2019, **15**(3), 432-439. doi:10.1016/j.dt.2018.12.002.
4. Kerr, C. & Ivey, P. An overview of the measurement errors associated with gas turbine aeroengine pyrometer systems. *J. Meas. Sci. Technol.*, 2002, **13**, 873. doi:10.1088/0957-0233/13/6/307.
5. Kerr, C. & Ivey, P. Optical pyrometry for gas turbine aeroengines. *Sensor Review*, 2004, **24**(4), 378 – 386. doi:10.1108/02602280410558412.
6. Moll, A. V.; Behbahani, A. R.; Fralick, G. C.; Wrbanek, J. D. & Hunter, G. W. A Review of Exhaust Gas Temperature Sensing Techniques for Modern Turbine Engine Controls. *In* 50<sup>th</sup> AIAA/ASME/SAE/ASEE Joint Propulsion Conference, July 2014, Cleveland, Ohio. doi:10.2514/6.2014-3977.
7. AGARD AR 320. Guide to the Measurement of Transient Performance of Aircraft Turbine Engines and Components. 1994, ISBN 92-835-0739-8.
8. Roga, S. CFD Analysis of scramjet engine combustion chamber with alternating wedge-shaped strut injector at flight mach 6.5. *J. Phys.: Conf. Series*, 2019, **1276**, 012038. doi: 10.1088/1742-6596/1276/1/012038.
9. Roga, S. CFD Analysis of scramjet engine combustion chamber with diamond-shaped strut injector at flight mach 4.5. *J. Phys.: Conf. Series*, 2019, **1276**, 012041. doi: 10.1088/1742-6596/1276/1/012041.
10. Pandey, K. M.; Roga S. & Choubey, G. Numerical investigation on hydrogen-fueled scramjet combustor with parallel strut fuel injector at a flight mach number of 6. *J. Applied Fluid Mech.*, 2016, **9**(3), 1215-1220. doi: 10.18869/acadpub.jafm.68.228.24082.
11. Ummer, Zahir; Weihao, Zhang; Weiping, Yang; Zhengping, Zou & Jian, Zhao. Numerical Investigation on Metrological Fidelity of a Shielded Thermocouple Probe and the Effects of Geometrical Parameters. *Int. J. Turbo Jet-Engines*, 2019. doi:10.1515/tjj-2019-0017.
12. Blachnio, J. & Pawlak, W. I. Damageability of Gas Turbine Blades – Evaluation of Exhaust Gas Temperature in Front of the Turbine Using a Non-Linear Observer. *Adv. Gas Turbine Technol.*, 2011, 435-464. doi: 10.5772/29546,
13. Mishra, R. K.; Elangovan, S. & Nagesh, U. Temperature Measurement Problems In An Aero Gas Turbine Engine. *In* Proceedings of International Conference on Instrumentation, INCON-2004, 19-21 Dec 2004, Pune, India.
14. Nunez-Cascajero, A.; Tapetado, A.; Vargas, S. & Vazquez, C. Optical fiber pyrometer designs for temperature measurements depending on object size. *Sensors*, 2021, **21**, 646. doi:10.3390/s21020646.
15. Paniagua, G.; Dénos, R. & Oropesa, M. Thermocouple probes for accurate temperature measurements in short duration facilities. *In* Proceedings of ASME Turbo Expo 2002, GT-2002-30043, 3-6 June 2002, Amsterdam, The Netherlands.
16. Zeisberger, Andreas. Total temperature probes for turbine and combustor applications. MTU Aero Engines GmbH, München, ISABE-2007-1108.
17. Bonham, C.; Thorpe, S. J.; Erlund, M. N. & Stevenson, R. J. Combination probes for stagnation pressure and temperature measurements in gas turbine engines. *J. Meas. Sci. Technol.*, 2017, **29**(1). doi:10.1088/1361-6501/aa925c.
18. ANSYS R14.5 Static Structural. ANSYS, Inc. July 2013. <https://www.ansys.com/en-in>
19. MIL-HDBK-1783B. Department Of Defense Handbook, Engine Structural Integrity Program (ENSIP). 15 Feb, 2002. [http://everyspec.com/MIL-HDBK/MIL-HDBK-1500-1799/MIL\\_HDBK\\_1783B\\_1924/](http://everyspec.com/MIL-HDBK/MIL-HDBK-1500-1799/MIL_HDBK_1783B_1924/)
20. ANSYS R19 Fluent. ANSYS, Inc. May 2019. <https://www.ansys.com/en-in>.
21. Lowery, G.W. & Vachon, R.I. The effect of turbulence on heat transfer from heated cylinders. *Int. J. Heat Mass Transfer*, 1975, **18**, 1229-1242.
22. Guide to thermocouple and resistance thermometry. TC Issue 6.1, 2012, U K.
23. Kim, C.S.; Hong, Sung-Deok; Seo, Dong-Un & Kim, Yong-Wan. Temperature Measurement with Radiation

Correction for Very High Temperature Gas. *In* 14<sup>th</sup> Int. Heat Transfer Conference, IHTC14-23074, Aug 8-13, 2010, Washington D. C., USA.  
doi: 10.1115/IHTC14-23074.

24. Saravanamuttoo, H. Recommended practices for measurement of gas path pressures and temperatures for performance assessment of aircraft turbine engines and components. Technical report, Defense Technical Information Centre, 1990, ISBN 92-835-0499-2.
25. Caldwell, F. R. Thermocouple materials. National Bureau of Standards Monograph 40, Mar 1969, Washington D. C., USA.
26. Nakos, J. T. Uncertainty Analysis of Thermocouple Measurements Used in Normal and Abnormal Thermal Environment Experiments at Sandia's Radiant Heat Facility and Lurance Canyon Burn Site. SANDIA REPORT, SAND2004-1023, 2004, Sandia National Laboratories, USA.

#### ACKNOWLEDGEMENTS

The authors are thankful to Instrumentation and Control Engineering group (ICG), Afterburner group, Heat transfer group (HTG) of GTRE for their valuable suggestions and constructive comments.

#### CONTRIBUTORS

**Mr Benny George** received his MTech from IIT Madras (Machine Design) and presently working as a scientist at DRDO- Gas Turbine Research Establishment, Bengaluru. He is currently involved in instrumentation of aero gas turbine engines. His research interest includes design and development of high temperature sensors and flight test instrumentation for aero gas turbine engines.

In the present work, he prepared the frame work for the study, carried out experimental work, result analysis and manuscript writing.

**Dr N. Muthuveerappan** received his PhD (CFD-Mechanical Engineering Department) from IIT Madras and currently he is project director at DRDO- Gas Turbine Research Establishment, Bengaluru. He has published many national and international papers. His area of research is in the field of combustion, afterburner and exhaust systems of aero gas turbine engines. He has been associated in guiding and reviewing the entire study.